

13th Deep Sea Offshore Wind R&D Conference, EERA DeepWind'2016, 20-22 January 2016, Trondheim, Norway

Rational upscaling of a semi-submersible floating platform supporting a wind turbine

Mareike Leimeister^{a,d,*}, Erin E. Bachynski^b, Michael Muskulus^c, Philipp Thomas^d

^aDepartment of Marine Technology, NTNU, NO-7491 Trondheim, Norway

^bCentre for Ships and Ocean Structures, NTNU, NO-7491 Trondheim, Norway

^cDepartment of Civil and Transport Engineering, NTNU, NO-7491 Trondheim, Norway

^dFraunhofer Institute for Wind Energy and Energy System Technology (IWES), D-27572 Bremerhaven, Germany

Abstract

This work examines the procedure of upscaling of a semi-submersible platform in order to support a predefined wind turbine. As a result of technological progress and design changes, basic scaling based on the turbine rating cannot be used directly. Furthermore, additional factors that floating structures have to deal with - like coupled dynamic motions, wave interaction, low frequency response and mooring system - have to be considered and included in the upscaling procedure. It is shown and discussed here, how to develop a rational upscaling process for a semi-submersible structure, under all these constraints, when the goal is to find a reasonable design of a platform, which would fit a predefined wind turbine, is producible, and has realistic dynamic behavior.

© 2016 The Authors. Published by Elsevier Ltd. This is an open access article under the CC BY-NC-ND license

(<http://creativecommons.org/licenses/by-nc-nd/4.0/>).

Peer-review under responsibility of SINTEF Energi AS

Keywords: Offshore wind energy; semi-submersible floating platform; upscaling; wind turbine

1. Introduction

Offshore wind energy has higher and more consistent wind resource potential, less size and noise limitations, and less visual impact than onshore wind energy. With floating wind turbines, promising sites at deeper water depths can be made accessible for the wind industry. Despite these advantages, the use of offshore wind power is still economically challenging because of higher installation and O&M costs, limited time windows for transport and installation, more difficult access, higher loads on the structure due to waves and current, and additional challenges like dynamic interaction between the floating structure and wind turbine or wave excitation frequencies.

One opportunity to reduce the costs is the installation of bigger but fewer wind turbines, which is more feasible offshore than onshore. Upscaling of smaller existing wind turbines to larger sizes is primarily based on geometric self-similarity. When aiming for the same optimal performance, similar aerodynamic behavior is needed and obtained by maintaining the tip speed ratio. The scaling factor is determined by the power rating and expressed in terms of

* Corresponding author. Tel.: +49-179-9843239.

E-mail address: mareike-leimeister@gmx.de

a length ratio. Due to the cubic increase in mass, however, buckling limit and yield strength are likely to limit the upscaling [1]. As the upscaling procedure does not consider Reynolds effects, wind shear, dynamic loads, and local or case-specific predefined constraints like noise limits or height requirements, existing wind turbines deviate from those theoretical scaling proportionalities [1]. By the same token, recent technology developments and new designs make simple geometrical upscaling insufficient. The support structure carrying the upscaled wind turbine also has to be adjusted, so that floatation and stability are maintained. Floating platforms are characterized by large coupled motions, low frequency modes, mooring system, and hydrodynamic interaction. As a consequence, simple upscaling based on the turbine rating cannot be applied in the case of floating offshore wind turbine systems.

This work examines the criteria that have to be fulfilled during upscaling of a semi-submersible floating system carrying a predefined wind turbine. Based on those factors, an adjusted upscaling procedure is developed, the resulting platform design is modelled, its hydrostatic and hydrodynamic parameters are determined, and its behavior is analyzed. As the main focus lies on the hydrodynamic behavior of the floating system and not on its structural integrity, structural scaling laws are not considered in this study. Section 2 covers the adjusted upscaling method and the derivation of system parameters. The results are presented in Section 3, divided into stability analysis, frequency-dependent behavior, natural periods and motion response. Finally, Section 4 provides recommendations for optimization and adaption of the upscaling procedure.

Nomenclature

A	Added mass matrix (6×6) with components A_{ii}	[kg, kgm, kgm ²]
B	Damping matrix (6×6) with components B_{ii}	[kg/s, kgm/s, kgm ² /s]
bot	Bottom end	
C	Stiffness matrix (6×6) with components C_{ii}	[kg/s ² , kgm/s ² , kgm ² /s ²]
CoB, CoG	Center of buoyancy, gravity	
<i>D</i>	Diameter	[m]
F	Excitation force vector (6×1) with components F_i	[N, Nm]
f_n	Natural frequency	[Hz]
<i>g</i>	Acceleration due to gravity	[m/s ²]
<i>I</i>	Area moment of inertia	[m ⁴]
<i>l</i>	Length	[m]
M	Mass matrix (6×6) with components M_{ii}	[kg, kgm, kgm ²]
RAO	Response amplitude operator	
S_q, S_η	Response/Wave spectral density	[m ²] or [deg ²]
<i>s</i>	Scaling factor	
T_d, T_n	(Damped) Natural period	[s]
top	Top end	
<i>W</i>	Weight	[N]
<i>x, y, z</i>	Coordinate and direction of surge, sway, heave	
ρ_{water}	Water density	[kg/m ³]
σ	Standard deviation	[m] or [deg]
ω	Angular frequency	[rad/s]

2. Methodology

The upscaling procedure was developed based on a case study: the OC4-DeepCwind semi-submersible floating platform [2], originally designed for the NREL 5 MW wind turbine, was modified to support Fraunhofer’s 7.5 MW wind turbine IWT-7.5-164 [3].

The main upscaling of the semi-submersible floating platform was based on the simple upscaling procedure with the geometrical scaling factor determined by the power rating of the wind turbines, as follows $s = \sqrt{\frac{7.5 \text{ MW}}{5 \text{ MW}}} \approx 1.225$,

since the power is proportional to a length scale (the rotor diameter) squared. However, the upscaling of the main column (MC) had to be adjusted, such that the main column fits the tower base diameter of 8.4 m. With the original main column diameter of 6.5 m a slightly higher scaling factor of $s \approx 1.292$ resulted for the main column diameter and wall thickness. The draft, however, was scaled with the main scaling factor. The lengths of the cross braces (CB) and pontoons that interconnect the outer and main columns were determined from the geometrical arrangement. Another geometrical boundary condition was the hub height of 120 m, for which the IWT-7.5 wind turbine was designed. In order to avoid changing the complex hybrid tower design, the main column was cut at SWL and it was assumed that the tower bottom, made out of concrete, could withstand wave impact.

The mooring system parameters (line length and anchor position) were assumed to be unchanged as well as the water depth of 200 m. Due to the upscaled fairlead positions, however, the suspended mooring line length changed and thus also the weight and center of gravity of the suspended parts. The latter two were computed based on [4], considering elastic catenary mooring lines.

Finally, the upscaled platform was ballasted with the main focus on floatability and stability. The buoyancy was predefined by the upscaled draft of the platform and the resulting displaced water volume. The weight of the upscaled platform, lifted mooring lines and wind turbine had to be complemented by ballast so that balance with buoyancy was achieved. With the main focus on stability, a low system center of gravity was desired, meaning that the base columns (BC) were ballasted first and the upper columns (UC) were filled with ballast only if needed. Two different designs were considered, one with water, as used in the original DeepCwind floater, and the other one with concrete, as it has a higher density than water, and thus a deeper center of gravity could be obtained.

Fig. 1 (a) visualizes the floating system, including the main criteria of the upscaling procedure. A top view of the floater with indication of the wave direction is presented in Fig. 1 (b).

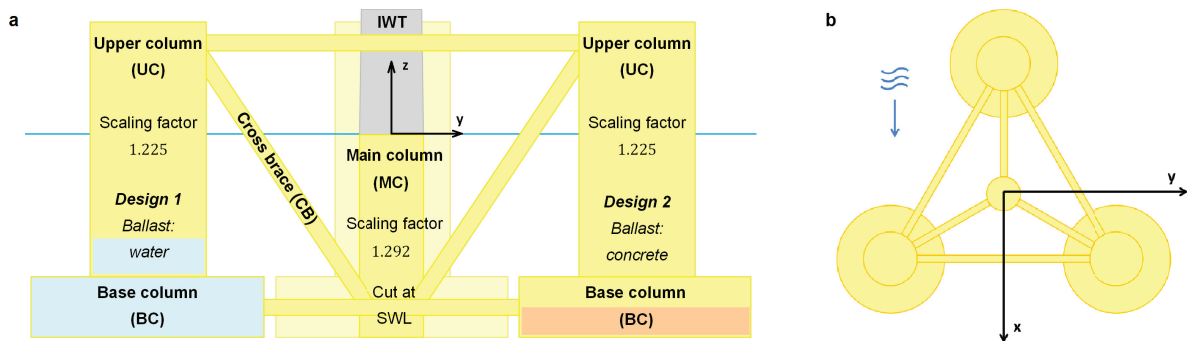


Fig. 1. (a) Components of the upscaled floating system; (b) Top view with coordinate system and wave direction

The theoretical scaling factor based on the power rating is not a strict rule. Comparisons of actual turbines suggest that the total tower top mass tends to scale with the power rating to 2 – 2.8 rather than 3, but there are uncertainties related to technological development [5]. In the case considered here, the nacelle mass increases at a higher rate due to the change from geared to direct drive. Similarly, there are uncertainties in the scaling of the loads due to the competing effects of tower height (reduced offshore) and extreme and fault loads (higher offshore).

The performance of the upscaled platform was analyzed based on hand calculations and computations by means of HydroD and Wadam by DNV GL. The focus lay on the stability limit in pitch, the natural periods, the nominal pitch at rated power, and the frequency-dependent behavior, considering only wave loads.

The simplified hand calculations used the wall-sided assumption in order to obtain the linear stiffness components of the system. The formulas for the hydrostatic components in heave and pitch are given in Equations 1 and 2, respectively. [6]

$$C_{33} = \rho_{\text{water}} g \frac{\pi}{4} \left[3 \left(D_{\text{UC}}^2 + D_{\text{CB}}^2 \frac{l_{\text{CB}}}{(z_{\text{top,CB}} - z_{\text{bot,CB}})} \right) + D_{\text{MC}}^2 \right] \quad (1)$$

$$C_{55} = W(z_{\text{CoB}} - z_{\text{CoG}}) + \rho_{\text{water}} g I_y \quad (2)$$

Besides the system stiffness, also the added mass had to be determined. For the hand calculations, two approaches were used. The first approximation was based on Equations 3 and 4 for heave and pitch, respectively [7,8]. Another approximation was obtained by scaling the given added mass values of the DeepCwind floating platform with the main scaling factor of $s \approx 1.225$ to the power of three for the heave DoF and to the power of five for pitch, neglecting the different scaling of the main column.

$$A_{33} = \frac{\rho_{\text{water}}}{6} D_{\text{MC}}^3 + 3 \left\{ \frac{\rho_{\text{water}}}{3} D_{\text{BC}}^3 - \left[\frac{\pi \rho_{\text{water}}}{8} D_{\text{UC}}^2 \left(D_{\text{BC}} - \sqrt{D_{\text{BC}}^2 - D_{\text{UC}}^2} \right) + \frac{\pi \rho_{\text{water}}}{24} \left(D_{\text{BC}} - \sqrt{D_{\text{BC}}^2 - D_{\text{UC}}^2} \right)^2 \left(2D_{\text{BC}} + \sqrt{D_{\text{BC}}^2 - D_{\text{UC}}^2} \right) \right] \right\} \quad (3)$$

$$A_{55} = 3\rho_{\text{water}} \frac{\pi}{4} D_{\text{BC}}^2 \left(\frac{|z_{\text{bot,BC}}|^3}{3} + (z_{\text{CoG,BC}} - z_{\text{bot,BC}})^2 |z_{\text{bot,BC}}| + (z_{\text{CoG,BC}} - z_{\text{bot,BC}}) |z_{\text{bot,BC}}|^2 \right) + \rho_{\text{water}} \frac{\pi}{4} D_{\text{MC}}^2 \left(\frac{|z_{\text{bot,MC}}|^3}{3} + (z_{\text{CoG,MC}} - z_{\text{bot,MC}})^2 |z_{\text{bot,MC}}| + (z_{\text{CoG,MC}} - z_{\text{bot,MC}}) |z_{\text{bot,MC}}|^2 \right) \quad (4)$$

Based on the simplified hand calculations only the undamped natural periods could be computed, not accounting for the cross-diagonal coupling and using the determined low-frequency limit of the added mass. In the natural period calculation based on the HydroD results, the frequency-dependency of added mass, however, was taken into account. Furthermore, by including the damping terms obtained by Wadam calculations, the damped natural periods could be computed based on Equation 5. The Wadam calculations included linearized drag forces based on Morison’s equation. The viscous drag forces are significantly smaller than the inertia forces due to the low Keulegan-Carpenter number of the considered flow conditions. Nonetheless, the contribution of the linearized viscous damping terms is important for the resonant response and is therefore included in the total damping matrix. In the present work, a simplification was made: the damping matrix was generated based on unit wave amplitude and was not updated for different sea states.

$$T_{d,i} = \left(f_{n,i} \sqrt{1 - \left(\frac{B_{ii}(f_{n,i})}{(M_{ii} + A_{ii}(f_{n,i})) 4\pi f_{n,i}} \right)^2} \right)^{-1} \quad \text{with} \quad f_{n,i} = \frac{1}{T_{n,i}} = \frac{1}{2\pi} \sqrt{\frac{C_{ii}}{M_{ii} + A_{ii}(f_{n,i})}} \quad (5)$$

3. Results

3.1. Stability analysis

As offshore wind turbines are facing the wind at high hub heights, but are supported by platforms with rather small footprints, attention has to be paid to the stability in pitch motion. Only considering static stability, the stability limit can be determined based on the location of the center of gravity with respect to the metacenter for different tilt angles. The stability limit can directly be taken from the righting lever GZ-curve as the first zero crossing point, which comes after the zero crossing point at the initial stable position. The main parameters of this static stability analysis are schematically visualized in Fig. 2.

This method is generally valid, but quite complex, so that computer programs have to be used or simplifying assumptions have to be made. For the hand calculations, all system components are assumed to be fixed, meaning that the center of gravity will not move within the local coordinate system of the structure. Furthermore, the change in the displaced water volume due to tilting is neglected. Thus, only accounting for the pitch motion and neglecting the required vertical translation for meeting the force equilibrium for floatation, the simplified hand calculations yield stability within the entire range of -19.0° to 18.9° used for the calculations, based on the geometrical arrangement shown in Fig. 2.

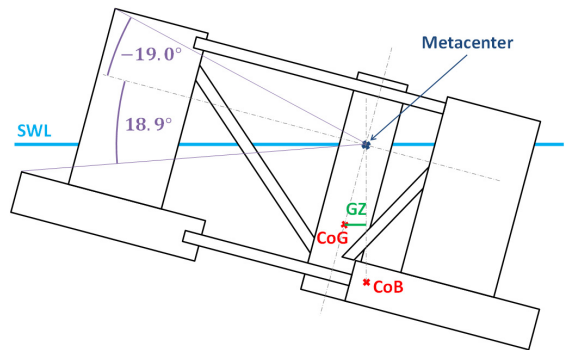


Fig. 2. Characteristic parameters and angles for the stability analysis

The more accurate stability analysis by means of HydroD shows that the stability limit is reached at a tilt angle of -73.2° for the water ballasted design and 92.8° for the concrete ballasted one. The maximum restoring force is achieved at -20° (and 30.0°) for both systems. Thus, the concrete ballasted design is more stable than the water ballasted one. This is as expected, since the center of gravity is lower.

3.2. Frequency-dependent hydrodynamic matrices

Based on the Wadam calculations, the frequency-dependent added mass and damping matrices were obtained, as shown in Fig. 3 (a) and (b). These matrices are independent of the ballasting. Due to symmetry, the surge and sway components, as well as the roll and pitch components, are the same.

In general, it is observed that the added mass in heave is much larger than in surge and sway, which is caused by the bigger base columns, acting as heave plates. At low frequencies, the added mass components in surge, sway and yaw reach around half of the double-body added mass, while the added mass components in heave, roll and pitch are not correlated with the double-body added mass values, as it is expected based on [9]. At higher frequencies, the added mass curves converge to a limit value. Comparing the heave and pitch low-frequency added mass limits with the hand calculated added mass components based on Equations 3 and 4, shown as dotted lines in Fig. 3 (a), confirms that the equation-based computations are only rough approximations, as they underestimate the results by 13 – 22%. The alternative of scaling up the original DeepCwind added mass components with the main scaling factor and just neglecting the different scaling of the main column, yields more accurate results, which still differ by 4.1 – 5.6% from the Wadam results.

The radiation damping curves, presented in Fig. 3 (b), show expected behavior, with the damping terms tending to approach zero at both small and high frequencies. The amount of damping in surge and sway is significantly higher than in heave. The same applies to the damping in yaw compared to roll and pitch. This is reasonable due to the geometry.

For semi-submersible platforms with large base columns, additional attention must be paid to the hydrodynamic excitation and damping on these columns. In the present work, viscous excitation has not been examined in detail. Simplified linearized viscous damping is included, but detailed analysis of the flow around the base plates is needed in order to correctly account for these effects. [10]

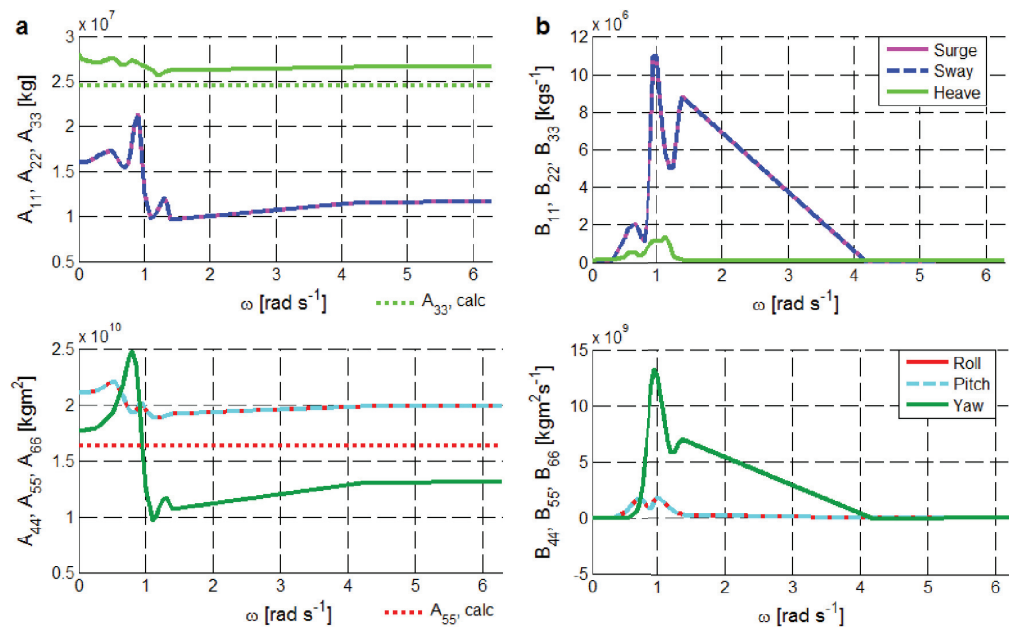


Fig. 3. (a) Diagonal added mass matrix terms; (b) Diagonal damping matrix terms.

3.3. Natural periods

As the hand calculations do not provide the system parameters, especially the added mass components, exactly, the damped natural periods were computed based on Equation 5 using the Wadam results and considering the frequency-dependency of the added mass and damping components. In order to include the station-keeping system in a first approach, the mooring stiffness of the catenary lines, directly taken from the original DeepCwind system [2], was added in the surge and yaw DoFs to the system stiffness. This way, the damped natural periods in surge, heave, pitch and yaw were computed explicitly. The results for both designs are presented in Table 1 together with the theoretical upscaled values of the original DeepCwind floating system (factor of \sqrt{s}), based on free decay load cases [11].

Table 1. Damped natural periods, given in s.

DoF	Water ballasted	Concrete ballasted	Theoretical upscaled	Original DeepCwind
Surge	153.6	153.6	118.2	106.8
Heave	19.1	19.1	19.1	17.3
Pitch	34.1	31.4	29.9	27.0
Yaw	131.4	131.7	83.8	75.7

From Table 1 it can be seen that the damped natural period in heave lies at the lower bound of the typical range for semi-submersible platforms (17-40 s, [12]), but is considerably higher than the natural period in heave of the original DeepCwind floating system, and follows the theoretical scaling.

As the concrete ballasted design is the stiffer system, the damped natural period in pitch is smaller than in the water ballasted system. Both values lie in the lower region of the typical natural periods in pitch of a semi-submersible platform (25-50 s, [12]) and are higher than the theoretical upscaled value, because of the ballasting from bottom up.

The damped natural periods in surge and yaw are significantly higher than the theoretical upscaled values. As the stiffness components in surge and yaw are directly taken from the DeepCwind system without any scaling, the theoretical upscaled values should rather be based just on the mass and added mass proportionalities. Using a factor of $\sqrt{s^3}$ and $\sqrt{s^5}$ for the natural periods in surge and yaw, respectively, adjusted theoretical upscaled values (144.8 s and 125.7 s) closer to the computed values are obtained. The remaining difference is due to the fact that mass and added mass do not exactly scale with s^3 in surge and s^5 in yaw.

3.4. Motion response

The motion response can be represented by the response amplitude operator (RAO) as given in Equation 6, depending on the excitation \mathbf{F} , and presented in Fig. 4.

$$|\text{RAO}(\omega)| = \left| \left[\mathbf{C} + i\omega\mathbf{B}(\omega) - \omega^2(\mathbf{M} + \mathbf{A}(\omega)) \right]^{-1} \mathbf{F}(\omega) \right| \quad (6)$$

The RAOs for the translational DoFs are equal for both designs. From Fig. 4 (a) it can be observed that the heave RAO represents in a general way the typical behavior [9], with a damping-dependent peak at the heave natural frequency, a static behavior in the stiffness dominated low-frequency range and an inertia-dependent decrease to zero at infinitely high frequencies.

The RAOs for the rotational motions, presented in Fig. 4 (b) and (c), are slightly different for the two upscaled designs. Due to the fact that the concrete ballasted system is stiffer than the water ballasted one, the corresponding RAOs in the rotational DoFs are smaller in the static region below the system’s natural frequency. At the natural frequencies, however, the RAOs of both systems are expected to be equal due to the same amount of damping. The results obtained by Wadam cannot represent this behavior exactly as the discrete frequencies are not at the system’s natural frequencies. Above the natural frequencies, the RAOs of the two designs can barely be distinguished one from the other, as the mass matrix components in the rotational DoFs only differ by at most 4%.

The DoFs of highest response, in general, are surge, heave and pitch, as the wave excitation is in surge direction and these motions are coupled. The obtained responses in sway, roll and yaw are insignificant and purely numerical.

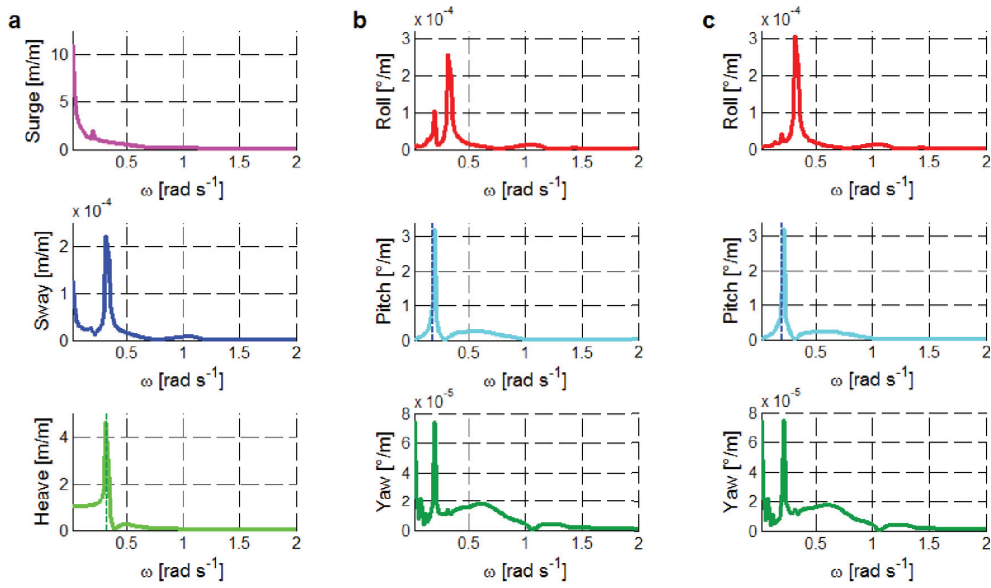


Fig. 4. RAOs in DoFs (a) 1 to 3 (both designs); (b) 4 to 6 (water ballasted); (c) 4 to 6 (concrete ballasted).

Based on 15 representative environmental conditions, response spectra ($S_q(\omega)$) and standard deviations (σ) of the motions were obtained, by means of Equation 7.

$$\sigma = \sqrt{\int_0^{\infty} S_q(\omega) d\omega} \quad \text{with} \quad S_q(\omega) = S_{\eta}(\omega) |\text{RAO}(\omega)|^2 \tag{7}$$

As the peak wave frequencies of the 15 conditions are beyond the system’s natural frequencies, there is almost no difference between the motion response of the two platform designs. The response spectra (not shown) are thus mainly affected by the wave excitation and not by the system’s eigenfrequencies, as the peak of the spectra occurs always at the peak wave frequency. The influence of the different significant wave heights is also only marginal compared to the peak wave frequencies. From the standard deviations of the motions, presented in Fig. 5, it can

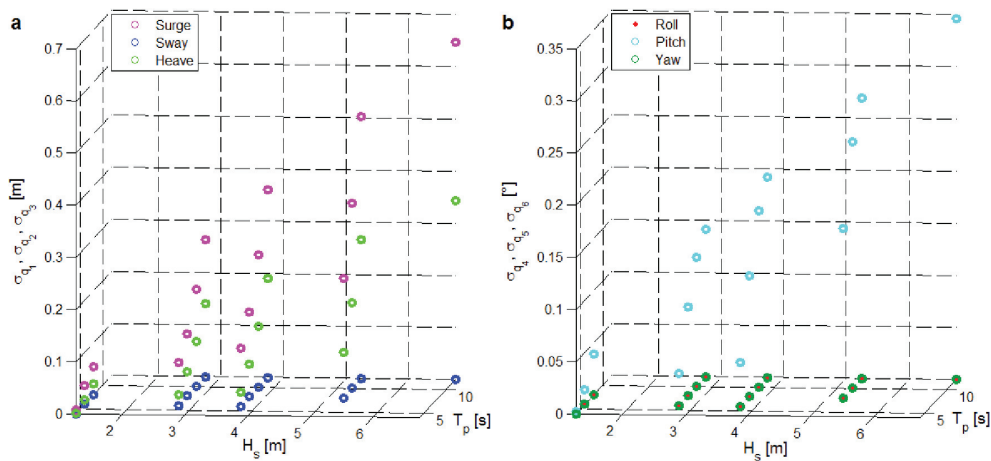


Fig. 5. Standard deviations in DoFs (a) 1 to 3; (b) 4 to 6.

be observed that the highest dynamic response occurs in surge, heave and pitch due to the directionality of the wave excitation, indicated in Fig. 1 (b). More severe environmental conditions also cause higher dynamic response. But still, the dynamic motions are quite small: at most 0.65 m in surge, 0.34 m in heave, and 0.34° in pitch. Comparing the dynamic response of both designs with different ballast systems shows that there is almost no difference for the considered environmental conditions, based on this linear frequency-domain analysis.

3.5. Nominal pitch displacement

As a proxy for the mean displacement of the floating wind turbine, the nominal pitch at maximum thrust was determined. The thrust force is the highest at rated wind speed and results with the hub height as lever arm in a moment in pitch of $1.386\text{E}+8$ Nm for the IWT-7.5-164 wind turbine [3]. Neglecting coupling terms, the nominal pitch displacement can be obtained by dividing the moment by the stiffness component in pitch. Due to the fact that this calculation is based on the static response and only includes the stiffness matrix, which is almost the same for the hand calculations and Wadam results, the obtained nominal pitch values are also comparable. As the concrete ballasted system is stiffer than the water ballasted one, the nominal pitch for the system with concrete as ballast (3.03°) is smaller than for the system with water as ballast (3.67°). Both values, however, are significantly higher than the theoretical upscaled nominal pitch displacement (2.31°) of the original DeepCwind floater, as the thrust force and corresponding moment cannot be compared directly for the two different turbine designs.

Comparing this maximum mean displacement with the standard deviations due to waves, it can be observed that the maximum dynamic pitch motion, occurring at the most severe sea state, is around 10% of the mean pitch displacement due to the maximum rotor thrust at rated wind speed.

4. Conclusion and outlook

In this work an initial upscaling of the OC4-DeepCwind semi-submersible floating platform was performed, such that Fraunhofer's wind turbine IWT-7.5-164 can be supported. Two upscaled floating platforms were designed with the focus on hydrodynamic performance, and compared regarding their static properties and dynamic behavior.

The high stability limits of -73.2° (water ballasted) and 92.8° (concrete ballasted), obtained by HydroD, indicate that both upscaled systems are too conservatively designed with respect to stability. A more detailed stability analysis including the mooring system and tower geometry is recommended.

The damped natural period in heave (19.1 s) is on the lower side of the typical range for semi-submersible platforms. Therefore, it is recommended to adjust the geometry such that the natural period in heave is increased. The water ballasted system yields a natural pitch period (34.1 s) more beyond the wave excitation than the concrete ballasted system (31.4 s), and is thus preferred from a frequency point of view. Due to the high stability limits, there is even room to increase the natural periods by elevating the center of gravity. Comparison with the original DeepCwind floating platform yields that both upscaled designs have higher natural periods, which is an advantageous aspect of upscaling. If the natural periods of the original DeepCwind floater are scaled up with the square root of the main scaling factor, however, it is found that the pitch natural frequency performance is better and the heave natural frequency performance is the same. The damped natural periods in surge and yaw are higher than the adjusted theoretical upscaled values. A more detailed analysis including the entire and exact mooring system stiffness is strongly recommended.

The maximum static pitch displacement at rated power is quite small (water: 3.67° , concrete: 3.03°), but - due to the different wind turbine designs - higher compared to the original DeepCwind floating system. Even in an extreme (fault) condition with a mean aerodynamic load of twice the rated load, the pitch displacement would still stay below the typical maximum allowable operational pitch of 10° . The dynamic motion is similar for both upscaled designs with a maximum of 0.65 m in surge, 0.34 m in heave and 0.34° in pitch.

For an optimized upscaling procedure, different scaling factors should be used for each component (smaller scaling factor for the upper columns, larger one for the base columns), in order to achieve higher natural frequencies in heave. This inhomogeneous scaling would most likely also influence the amount of displaced water volume. Thus, also adjustment of the amount of ballast and a change in the resulting total system mass, as well as the influence on the

stiffness in pitch and system's stability have to be considered in the optimization. The ballast system of the platform should be chosen such that an optimized balance between stability and natural frequencies further outside the wave excitation is found. Furthermore, the mooring system has to be analyzed more in detail and parameters like total length or location of the anchors have to be adjusted if needed.

Acknowledgements

This work has been partly supported by NOWITECH FME (Research Council of Norway, contract no. 193823). The authors also wish to acknowledge the financial support from Research Council of Norway through Center for Ships and Ocean Structures (CeSOS) and Centre for Autonomous Marine Operations and Systems (AMOS, RCN Project number 223254).

References

- [1] Sieros, G.; Chaviaropoulos, P.; Sørensen, J.D.; Bulder, B.H. and Jamieson, P. (2012). Upscaling Wind Turbines: theoretical and practical aspects and their impact on the cost of energy. *Wind Energy*, 15(1):3-17.
- [2] Robertson, A.; Jonkman, J.; Masciola, M.; Song, H.; Goupee, A.; Coulling, A. and Luan, C. (2014). Definition of the Semisubmersible Floating System for Phase II of OC4. Technical Report NREL/TP-5000-60601, NREL.
- [3] Sevinc, A.; Rosemeier, M.; Bätge, M.; Braun, R.; Meng, F.; Shan, M.; Horte, D.; Balzani, C. and Reuter, A. (2015). IWES Wind Turbine IWT-7.5-164 Specification, Revision 02. Data Sheet, Fraunhofer Institute for Wind Energy and Energy System Technology, Leibniz University Hanover - Institute of Wind Energy Systems.
- [4] Monarcha, A. and Fonseca, N. (2012). A static analytical method for the preliminary design of multiple line mooring systems. In Santos, T.A.; Soares, C.G.; Garbatov, Y. and Sutulo, S., *Maritime Engineering and Technology*, pages 195-203. CRC Press.
- [5] Jamieson, P. (2011). *Innovation in Wind Turbine Design*. John Wiley & Sons, Ltd, 1st edition.
- [6] Bredmose, H. (2014). Floating Wind Turbines. Presentation within the course "Offshore Wind Energy", Technical University of Denmark, Department of Wind Energy.
- [7] Tao, L. and Cai, S. (2004). Heave motion suppression of a Spar with a heave plate. *Ocean Engineering*, 31:669-692.
- [8] Ghadimi, P.; Bandari, H.P. and Rostami, A.B. (2012). Determination of the Heave and Pitch Motions of a Floating Cylinder by Analytical Solution of its Diffraction Problem and Examination of the Effects of Geometric Parameters on its Dynamics in Regular Waves. *International Journal of Applied Mathematical Research*, 1(4):611-633.
- [9] Newman, J.N. (1977). *Marine Hydrodynamics*. The MIT Press.
- [10] Benitz, M.A.; Schmidt, D.P.; Lackner, M.A.; Stewart, G.M.; Jonkman, J. and Robertson, A. (2015). Validation of Hydrodynamic Load Models using CFD for the OC4-DeepCwind Semisubmersible. Proceedings of the ASME 2015 34th International Conference on Ocean, Offshore and Arctic Engineering, St. John's, Newfoundland, Canada. Volume 9: Ocean Renewable Energy, V009T09A037.
- [11] Robertson, A.; Jonkman, J.; Vorpahl, F.; Popko, W.; et al. (2014). Offshore Code Comparison Collaboration Continuation Within IEA Wind Task 30: Phase II Results Regarding a Floating Semisubmersible Wind System. ASME 2014 33rd International Conference on Ocean, Offshore and Arctic Engineering, San Francisco, California, USA. Volume 9B: Ocean Renewable Energy, V09BT09A012.
- [12] Yu, Q. and Chen, X. (2013). Contract E12PC00027: Design Guideline for Stationkeeping Systems of Floating Offshore Wind Turbines, Final Report. American Bureau of Shipping (ABS).